

Search for lepton portal dark matter in the PandaX-4T experiment

Xuyang Ning,² Zihao Bo,² Wei Chen,² Xun Chen,^{1,2,3,4} Yunhua Chen,^{5,4} Zhaokan Cheng,⁶ Xiangyi Cui,¹ Yingjie Fan,⁷ Deqing Fang,⁸ Zhixing Gao,² Lisheng Geng,^{9,10,11,12} Karl Giboni,^{2,4} Xunan Guo,⁹ Xuyuan Guo,^{5,4} Zichao Guo,⁹ Chencheng Han,¹ Ke Han,^{2,4} Changda He,² Jinrong He,⁵ Di Huang,² Houqi Huang,¹³ Junting Huang,^{2,4} Ruquan Hou,^{3,4} Yu Hou,¹⁴ Xiangdong Ji,¹⁵ Xiangpan Ji,¹⁶ Yonglin Ju,^{14,4} Chenxiang Li,² Jiafu Li,¹⁷ Mingchuan Li,^{5,4} Shuaijie Li,^{5,2,4} Tao Li,⁶ Zhiyuan Li,⁶ Qing Lin,^{18,19} Jianglai Liu,^{1,2,3,4,*} Congcong Lu,¹⁴ Xiaoying Lu,^{20,21} Lingyin Luo,²² Yunyang Luo,¹⁹ Wenbo Ma,² Yugang Ma,⁸ Yajun Mao,²² Yue Meng,^{2,3,4} Binyu Pang,^{20,21} Ningchun Qi,^{5,4} Zhicheng Qian,² Xiangxiang Ren,^{20,21} Dong Shan,¹⁶ Xiaofeng Shang,² Xiyuan Shao,¹⁶ Guofang Shen,⁹ Manbin Shen,^{5,4} Wenliang Sun,^{5,4} Yi Tao,^{2,3} Anqing Wang,^{20,21} Guanbo Wang,² Hao Wang,² Jiamin Wang,¹ Lei Wang,²³ Meng Wang,^{20,21} QiuHong Wang,⁸ Shaobo Wang,^{2,13,4} Siguang Wang,²² Wei Wang,^{6,17} Xiuli Wang,¹⁴ Xu Wang,¹ Zhou Wang,^{1,2,3,4} Yuehuan Wei,⁶ Weihao Wu,^{2,4} Yuan Wu,² Mengjiao Xiao,² Xiang Xiao,¹⁷ Kaizhi Xiong,^{5,4} Yifan Xu,¹⁴ Shunyu Yao,¹³ Binbin Yan,¹ Xiyu Yan,²⁴ Yong Yang,^{2,4} Peihua Ye,² Chunxu Yu,¹⁶ Ying Yuan,² Zhe Yuan,⁸ Youhui Yun,² Xinning Zeng,² Minzhen Zhang,¹ Peng Zhang,^{5,4} Shibo Zhang,¹ Shu Zhang,¹⁷ Tao Zhang,^{1,2,3,4} Wei Zhang,¹ Yang Zhang,^{20,21} Yingxin Zhang,^{20,21} Yuanyuan Zhang,¹ Li Zhao,^{1,2,3,4} Jifang Zhou,^{5,4} Jiaxu Zhou,¹³ Jiayi Zhou,¹ Ning Zhou,^{1,2,3,4,†} Xiaopeng Zhou,⁹ Yubo Zhou,² and Zhizhen Zhou²
(PandaX Collaboration)

Yang Bai^{25,‡}

- ¹New Cornerstone Science Laboratory, Tsung-Dao Lee Institute, Shanghai Jiao Tong University, Shanghai 201210, China
²School of Physics and Astronomy, Shanghai Jiao Tong University, Key Laboratory for Particle Astrophysics and Cosmology (MoE), Shanghai Key Laboratory for Particle Physics and Cosmology, Shanghai 200240, China
³Shanghai Jiao Tong University Sichuan Research Institute, Chengdu 610213, China
⁴Jinping Deep Underground Frontier Science and Dark Matter Key Laboratory of Sichuan Province, Liangshan 615000, China
⁵Yalong River Hydropower Development Company, Ltd., 288 Shuanglin Road, Chengdu 610051, China
⁶Sino-French Institute of Nuclear Engineering and Technology, Sun Yat-Sen University, Zhuhai 519082, China
⁷Department of Physics, Yantai University, Yantai 264005, China
⁸Key Laboratory of Nuclear Physics and Ion-beam Application (MOE), Institute of Modern Physics, Fudan University, Shanghai 200433, China
⁹School of Physics, Beihang University, Beijing 102206, China
¹⁰Peng Huanwu Collaborative Center for Research and Education, Beihang University, Beijing 100191, China
¹¹International Research Center for Nuclei and Particles in the Cosmos & Beijing Key Laboratory of Advanced Nuclear Materials and Physics, Beihang University, Beijing 100191, China
¹²Southern Center for Nuclear-Science Theory (SCNT), Institute of Modern Physics, Chinese Academy of Sciences, Huizhou 516000, China
¹³SJTU Paris Elite Institute of Technology, Shanghai Jiao Tong University, Shanghai 200240, China
¹⁴School of Mechanical Engineering, Shanghai Jiao Tong University, Shanghai 200240, China
¹⁵Department of Physics, University of Maryland, College Park, Maryland 20742, USA
¹⁶School of Physics, Nankai University, Tianjin 300071, China
¹⁷School of Physics, Sun Yat-Sen University, Guangzhou 510275, China
¹⁸State Key Laboratory of Particle Detection and Electronics, University of Science and Technology of China, Hefei 230026, China
¹⁹Department of Modern Physics, University of Science and Technology of China, Hefei 230026, China
²⁰Research Center for Particle Science and Technology, Institute of Frontier and Interdisciplinary Science, Shandong University, Qingdao 266237, China
²¹Key Laboratory of Particle Physics and Particle Irradiation of Ministry of Education, Shandong University, Qingdao 266237, China
²²School of Physics, Peking University, Beijing 100871, China
²³College of Nuclear Technology and Automation Engineering, Chengdu University of Technology, Chengdu 610059, China
²⁴School of Physics and Astronomy, Sun Yat-Sen University, Zhuhai 519082, China
²⁵Department of Physics, University of Wisconsin-Madison, WI 53706, USA

(Dated: August 28, 2024)

We report a search for a lepton-portal dark matter model, where dark matter couples to a charged lepton in the standard model. This simplified model naturally leads to photon-mediated dark matter interactions with nuclei, making it suitable for direct dark matter detection experiments. Matching to the framework of non-relativistic effective field theory for dark matter, we report the first sensitive search for this model using data from the PandaX-4T commissioning run. Our results yield strong constraints on Dirac fermion dark matter but relatively weaker constraints on Majorana dark matter

due to the suppression of effective photon interactions. These constraints complement those obtained from the collider and indirect detection experiments.

Plenty of astronomical and cosmological observations indicate the existence of dark matter (DM) [1], but the nature of DM remains unknown. It is usually assumed that DM is made up of non-baryonic, neutral and fundamental particles. However, there are still some possibilities that dark matter possesses minute electromagnetic couplings with photons which evades the current experimental constraints. Recently, we reported a search of DM's electromagnetic properties with the PandaX-4T experiment [2], which uses the effective field theory (EFT) approach and provides constraints on individual photon-mediated operators. It turns out that the most stringent constraint on the charge radius square of DM is stronger than that of the neutrinos by approximately four orders of magnitude. To understand the origin of these possible electromagnetic properties, we need to go beyond the EFT theory to the ultraviolet (UV)-complete theories. A generic UV-complete model, running down to low-energy scales, will generally give rise to multiple types of EFT operators simultaneously. In addition, DM searches with collider experiments, especially those conducted at the Large Hadron Collider (LHC), are performed at significant higher energy scale where the validity of EFT may break down. Therefore, a UV-complete model is necessary to combine the results from direct detection, indirect detection and collider searches.

In this work, our focus is on one specific realization of photon-mediated interaction: the lepton-portal DM (LPDM) model [3–5]. The general construction involves assuming a portal coupling between the dark sector and standard model (SM) leptons. Usually, a neutral DM candidate χ and a charged scalar mediator with a heavier mass are assumed in the dark sector. This model is gaining increasing attentions due to the additional loop contributions from the dark sector and its potential to explain the muon anomalous magnetic moment [5–8]. In direct DM detection experiments, this model can naturally generate the photon-mediated loop process between DM candidates and the target nuclei. This process can be expressed within the framework of DM EFT approach by matching it to the relevant effective operators. In this letter, we perform a sensitive search for the LPDM using the EFT treatment with the data from PandaX-4T commissioning run for the first time.

In the LPDM, within a minimal setup, two new particles in the dark sector are introduced. The lighter one is the DM candidate, while the other serves as a charged mediator facilitating interactions between DM and SM leptons. In the minimal model, the dark sector exclusively couples to the right-handed SM lepton [4]. Depending on the nature of the DM candidate, the forms of photon-mediated interactions and their corresponding

signatures in direct detection experiments vary. In this work, our focus is on the scenario where DM is a fermion, either Dirac or Majorana, and the interaction is mediated by an $SU(2)_L$ singlet particle.

The corresponding Lagrangian for a fermion DM in LPDM is:

$$\mathcal{L}_{\text{LPDM}} \supset \lambda_i \phi_i \bar{\chi}_L e_R^i + h.c. \quad (1)$$

The free parameters include the charged mediator ϕ mass m_ϕ , DM mass m_χ , and the coupling λ_i to a specific lepton flavor i . To avoid any flavor violating process from the dark sector, we assume that the coupling occurs exclusively with a single SM lepton in the mass eigenstate at any given time. As an example, we take muon as the only portal-linked lepton particle in this work. This scenario offers a possibility to address phenomena such as the muon magnetic anomaly [9].

In direct detection, since the dark sector interacts exclusively with charged leptons, the leading contribution to DM scattering off a nucleus is a loop process mediated by photon. The relevant Feynman diagrams induced by photon are shown in Fig. 1. Additional diagrams induced

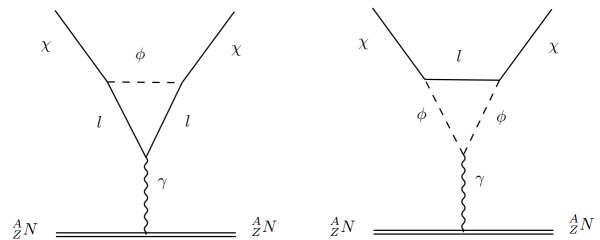


FIG. 1. Feynman diagrams contributing to the photon-mediated interaction between DM and the nucleus at the loop level.

by Z or Higgs boson are also possible, but they are subdominant compared to the electromagnetic moments and can be neglected safely [10].

The photon-mediated process contains multipole effective interactions,

$$\begin{aligned} \mathcal{L}_{\text{LPDM}} &= \mathcal{L}_{\text{CR}} + \mathcal{L}_{\text{MD}} + \mathcal{L}_{\text{A}} + \mathcal{L}_{\text{ED}} \\ &= b_\chi \bar{\chi} \gamma^\mu \chi \partial^\nu F_{\mu\nu} + \frac{\mu_\chi}{2} \bar{\chi} \sigma^{\mu\nu} \chi F_{\mu\nu} \\ &\quad + a_\chi \bar{\chi} \gamma^\mu \gamma^5 \chi \partial^\nu F_{\mu\nu} + i \frac{d_\chi}{2} \bar{\chi} \sigma^{\mu\nu} \gamma^5 \chi F_{\mu\nu}, \end{aligned} \quad (2)$$

where b_χ , μ_χ , a_χ and d_χ are the Wilson coefficients corresponding to DM charge radius (CR), magnetic dipole (MD), anapole (A), and electric dipole (ED) moments. The values of these coefficients are determined by the LPDM parameters, and their renormalization group evolution results in a logarithmic enhancement, as shown

in the Appendix. These relativistic effective operators lead to interactions between DM and nuclei mediated by photons. For the Dirac fermion DM case, interactions through the charge radius b_χ and the magnetic dipole μ_χ are particularly significant, while the anapole moment a_χ is suppressed, and the electric dipole moment d_χ vanishes in this simple setup. For Majorana fermion DM, only the anapole moment a_χ is non-vanishing. As seen here, this UV-complete model leads to various types of relativistic operators and their mixing, making it challenging to directly translate constraints from a single operator.

In the non-relativistic limit for direct detection, these photon-mediated interactions are further matched to linear combinations of non-relativistic EFT (NREFT) operators [11]. These NREFT operators are constructed based on parameters such as the momentum exchange q , DM velocity v , DM spin S_χ , and nucleon spin S_N [12–14], shown in Appendix for details. Utilizing the corresponding Wilson coefficients and relevant effective operators, the differential event rate in the xenon detector can be derived using DMFormFactor [11, 15], which incorporates the xenon nuclear response functions from comprehensive full-basis shell-model calculations. The nuclear recoil (NR) energy spectrum of a xenon nucleus in LPDM is shown in Fig. 2. In the case of Majorana fermion DM, the DM scattering cross section is suppressed by the DM velocity or NR energy E_R , resulting in a small predicted signal rate.

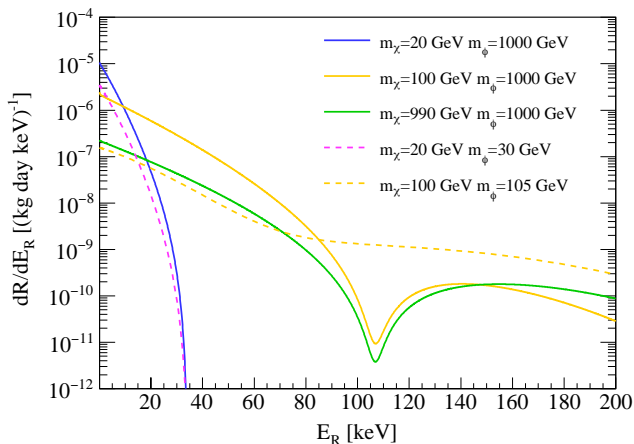


FIG. 2. Differential event rate as a function of nuclear recoil energy E_R for lepton portal DM scattering off a xenon nucleus, assuming a coupling $\lambda = 1$. Different DM masses and mediator masses are shown in various colors. Solid lines are for the Dirac fermion DM, while dashed lines are for the Majorana fermion DM.

The PandaX-4T experiment, located in the B2 hall of the China Jinping Underground Laboratory (CJPL), operates a dual-phase time projection chamber (TPC) with 3.7 tonne liquid xenon in the sensitive volume, aiming to explore new physics related to both DM and neutrinos.

Prompt scintillation light ($S1$) and delayed electroluminescence photons from ionized electrons ($S2$) of a scattering event are collected by two arrays of 3-inch photomultiplier tubes (PMTs). The 3-dimensional scattering position is reconstructed using the time difference between $S1$ and $S2$ in the z-direction, along with the $S2$ top PMT patterns in the x-y direction. The deposited energy is reconstructed based on the charge of $S1$ and $S2$. The signal response model in PandaX-4T follows the standard NEST v2.2.1 construction [16, 17], with parameters fitted from the low-energy calibration data which were taken at the end of run.

The data used to search for the LPDM correspond to an 86.0 live-day exposure during the PandaX-4T commissioning run. The event selection criteria follow the analysis for WIMP searches [18], with the region of interest (ROI) defined as $S1$ ranging from 2 to 135 photoelectrons (PEs) and raw $S2$ from 80 to 20,000 PEs. A total of 1058 events are identified within the ROI, as shown in Fig 3. The expected number of events from the background is 1054 ± 39 , which includes sources such as tritium, ^{85}Kr , radon, material radioactivity, surface, ^{136}Xe , neutrons, neutrinos and accidental $S1 - S2$ coincidence events, as summarized in Ref. [18]. We construct a two-sided profile likelihood ratio to test the signal hypothesis, using the standard unbinned likelihood [19] along with Gaussian penalty terms to account for the uncertainty associated with each nuisance parameter. Probability density functions (PDFs) for both the background components and the signal are generated based on the signal response model in $S1$ versus $S2_b$ (bottom-only $S2$) space.

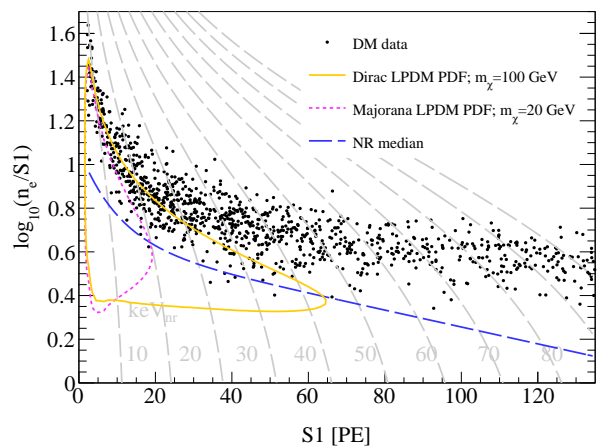


FIG. 3. The distribution of the final candidate events in PandaX-4T experiment in $\log_{10}(n_e/S1)$ vs. $S1$, where n_e is the number of ionized electrons. The green (magenta) line is the 2σ contour of the expected distribution of $100 \text{ GeV}/c^2$ Dirac LPDM ($20 \text{ GeV}/c^2$ Majorana LPDM) with mediator mass $m_\phi = 1 \text{ TeV}/c^2$ ($30 \text{ GeV}/c^2$) and coupling strength $\lambda = 1$. The dashed blue line is the fitted median of the nuclear recoil events from neutron calibration data.

The constraints on LPDM are shown in Fig 4, as a function of the DM mass m_χ and the mediator mass m_ϕ with a coupling strength $\lambda = 1$. It's important to note that, for the stability of DM, only the region where $m_\phi > m_\chi$ is allowed. For the Dirac fermion DM case, LPDM in collider experiments exhibits signature analogous to the pair production of right-handed sleptons from the Minimal Supersymmetric Standard Model (MSSM) [20, 21]. The latest constraints from the ATLAS slepton searches with two-lepton plus large missing transverse energy final state in 139 fb^{-1} of data are also included [22]. Direct detection provides compelling results across most of the plotted mass range. However, for DM masses less than $8 \text{ GeV}/c^2$, collider experiments present stronger constraints due to the decrease in efficiency for lower recoil energy regions in direct detection. Indirect detection experiments also contribute constraints due to the DM direct annihilation into leptons in LPDM. This includes measurements such as the positron fraction measurement by AMS-02 [23], as well as the indirect limits on $\langle\sigma v\rangle$ derived from FERMI observations of the Galactic Halo [24] and Milky Way Dwarf [25], as depicted in Fig 4. It's worth noting that our results exclude the parameter combinations of Dirac DM that would satisfy the thermal relic density. In the case of Majorana fermion DM, the constraints from direct detection are weaker due to velocity or recoil energy suppression, which leaves a substantial parameter space open to address the muon magnetic moment anomaly.

In summary, utilizing data from the PandaX-4T commissioning run, we conduct a search for a UV-complete lepton portal dark matter model, which introduces photon-mediated interactions between DM and nucleons. Constraints on the mediator and DM masses are derived, assuming a muon-only portal with $\lambda = 1$. Our findings provide the strongest constraints for the Dirac fermion DM and encompass the largest parameter space for Majorana fermion DM with DM masses exceeding $10 \text{ GeV}/c^2$. These results suggest that, for the UV complete model, direct detection offers promising constraint and can complement collider or indirect detection experiments, given their distinct advantages in different regions. The PandaX-4T experiment continues to collect physics data and will further explore these uncharted parameter spaces.

ACKNOWLEDGEMENT

We thank Wick Haxton, Zuowei Liu and Natsumi Nagata for helpful discussions. This project is supported in part by grants from National Science Foundation of China (Nos. 12090060, 12090061, 12325505, U23B2070), a grant from the Ministry of Science and Technology of China (Nos. 2023YFA1606200, 2023YFA1606201), and by Office of Science and Technology, Shanghai Municipal

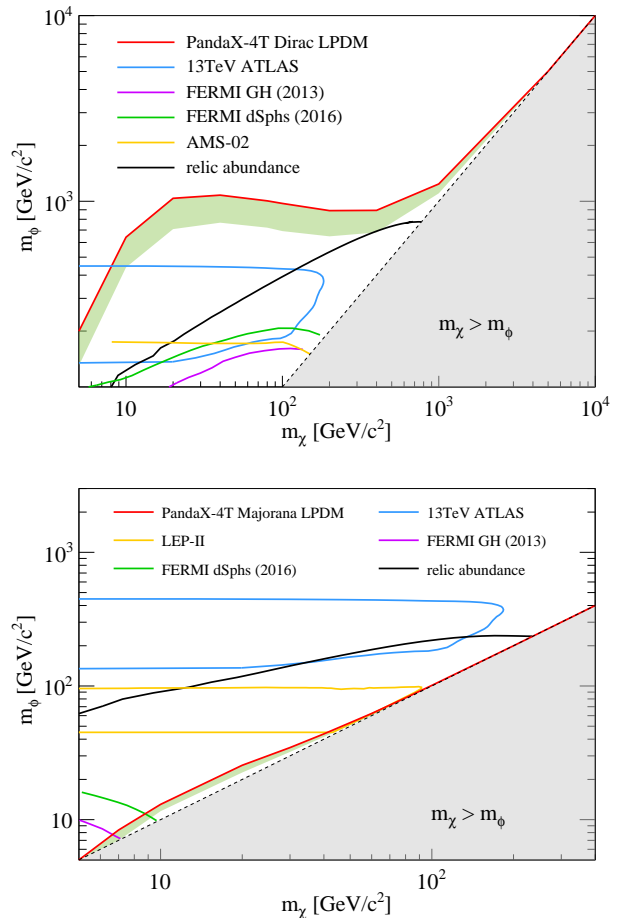


FIG. 4. Constraints on the mediator mass as a function of dark matter mass in the LPDM for both Dirac fermion DM (upper panel) and Majorana fermion DM (lower panel). The green band represents $\pm 1\sigma$ sensitivity band. A coupling strength of $\lambda = 1$ is assumed. The collider results are taken from the search for the right-handed slepton signals by the ATLAS experiment [22] and LEP-II experiment [26]. Indirect detection bounds are sourced from [3, 4]. Additionally, the parameter region for LPDM that satisfies the thermal relic density [4] is indicated, predominantly governed by the ϕ -mediated tree-level annihilation process.

Government (grant No. 22JC1410100, 21TQ1400218). We thank for the support by the Fundamental Research Funds for the Central Universities. We also thank the sponsorship from the Chinese Academy of Sciences Center for Excellence in Particle Physics (CCEPP), Hongwen Foundation in Hong Kong, New Cornerstone Science Foundation, Tencent Foundation in China, and Yangyang Development Fund. Finally, we thank the CJPL administration and the Yalong River Hydropower Development Company Ltd. for indispensable logistical support and other help.

Appendix

* Spokesperson: jianglai.liu@sytu.edu.cn

† Corresponding author: nzhou@sytu.edu.cn

‡ Corresponding author: yangbai@physics.wisc.edu

- [1] G. Bertone, D. Hooper, and J. Silk, *Phys. Rept.* **405**, 279 (2005), arXiv:hep-ph/0404175.
- [2] X. Ning *et al.* (PandaX), *Nature* **618**, 47 (2023).
- [3] B. J. Kavanagh, P. Panci, and R. Ziegler, *Journal of High Energy Physics* **2019** (2019), 10.1007/jhep04(2019)089.
- [4] Y. Bai and J. Berger, *Journal of High Energy Physics* **2014** (2014), 10.1007/jhep08(2014)153.
- [5] J. Kawamura, S. Okawa, and Y. Omura, *JHEP* **08**, 042 (2020), arXiv:2002.12534 [hep-ph].
- [6] Y. Bai and J. Berger, (2021), arXiv:2104.03301 [hep-ph].
- [7] J. Kawamura, S. Okawa, and Y. Omura, (2022), arXiv:2204.07022 [hep-ph].
- [8] J. Liu, X.-P. Wang, and K.-P. Xie, *JHEP* **06**, 149 (2021), arXiv:2104.06421 [hep-ph].
- [9] D. P. Aguillard *et al.* (Muon g-2), (2023), arXiv:2308.06230 [hep-ex].
- [10] A. Ibarra and S. Wild, *Journal of Cosmology and Astroparticle Physics* **2015**, 047–047 (2015).
- [11] A. L. Fitzpatrick, W. Haxton, E. Katz, N. Lubbers, and Y. Xu, *Journal of Cosmology and Astroparticle Physics* **2013**, 004–004 (2013).
- [12] E. Del Nobile, *Physical Review D* **98** (2018), 10.1103/physrevd.98.123003.
- [13] A. L. Fitzpatrick, W. Haxton, E. Katz, N. Lubbers, and Y. Xu, (2012), arXiv:1211.2818 [hep-ph].
- [14] F. Bishara, J. Brod, B. Grinstein, and J. Zupan, *JHEP* **11**, 059 (2017), arXiv:1707.06998 [hep-ph].
- [15] N. Anand, A. L. Fitzpatrick, and W. C. Haxton, *Physical Review C* **89** (2014), 10.1103/physrevc.89.065501.
- [16] M. Szydagis *et al.*, “Noble Element Simulation Technique v2.0,” (2018).
- [17] M. Szydagis *et al.*, *Instruments* **5**, 13 (2021).
- [18] Y. Meng *et al.* (PandaX-4T), *Phys. Rev. Lett.* **127**, 261802 (2021), arXiv:2107.13438 [hep-ex].
- [19] D. Baxter *et al.*, (2021), arXiv:2105.00599 [hep-ex].
- [20] M. W. Cahill-Rowley, J. L. Hewett, A. Ismail, and T. G. Rizzo, *Phys. Rev. D* **88**, 035002 (2013), arXiv:1211.1981 [hep-ph].
- [21] M. Cahill-Rowley, R. Cotta, A. Drlica-Wagner, S. Funk, J. Hewett, A. Ismail, T. Rizzo, and M. Wood, *Phys. Rev. D* **91**, 055011 (2015), arXiv:1405.6716 [hep-ph].
- [22] G. Aad *et al.* (ATLAS), *Eur. Phys. J. C* **80**, 123 (2020), arXiv:1908.08215 [hep-ex].
- [23] M. Aguilar *et al.* (AMS Collaboration), *Phys. Rev. Lett.* **110**, 141102 (2013).
- [24] M. Ackermann *et al.* (Fermi-LAT), *The Astrophysical Journal* **761**, 91 (2012).
- [25] M. Ackermann *et al.* (Fermi-LAT), *Phys. Rev. Lett.* **115**, 231301 (2015), arXiv:1503.02641 [astro-ph.HE].
- [26] “LEP SUSY Working Group (ALEPH, DELPHI, L3, OPAL). Notes LEPSUSYWG/01-03.1,04-01.1,” .
- [27] C. Arina, A. Cheek, K. Mimasu, and L. Pagani, *Eur. Phys. J. C* **81**, 223 (2021), arXiv:2005.12789 [hep-ph].

The photon-mediated relativistic effective operators can be matched to the linear combination of non-relativistic DM-nucleons operators [2, 3, 11–14, 27]:

$$\begin{aligned}
\mathcal{L}_{\text{MD}} &= \frac{\mu_\chi}{2} \bar{\chi} \sigma^{\mu\nu} \chi F_{\mu\nu} \\
&\rightarrow \mathcal{O}_{\text{MD}} = \mu_\chi \frac{8\pi^2}{2e} \left[-\frac{\alpha}{2\pi} Q_N \left(\frac{\mathcal{O}_1}{m_\chi} + 4 \frac{m_N}{q^2} \mathcal{O}_5 \right) \right. \\
&\quad \left. - \frac{\alpha}{\pi} \frac{g_N}{m_N} \left(\mathcal{O}_4 - \frac{m_N^2}{q^2} \mathcal{O}_6 \right) \right], \\
\mathcal{L}_{\text{ED}} &= i \frac{d_\chi}{2} \bar{\chi} \sigma^{\mu\nu} \gamma^5 \chi F_{\mu\nu} \\
&\rightarrow \mathcal{O}_{\text{ED}} = d_\chi \frac{8\pi^2}{2e} \frac{2\alpha}{\pi} \frac{m_N}{q^2} Q_N \mathcal{O}_{11}, \\
\mathcal{L}_{\text{A}} &= a_\chi \bar{\chi} \gamma^\mu \gamma^5 \chi \partial^\nu F_{\mu\nu} \\
&\rightarrow \mathcal{O}_{\text{A}} = e a_\chi (2Q_N \mathcal{O}_8 - g_N \mathcal{O}_9), \\
\mathcal{L}_{\text{CR}} &= b_\chi \bar{\chi} \gamma^\mu \chi \partial^\nu F_{\mu\nu} \\
&\rightarrow \mathcal{O}_{\text{CR}} = e b_\chi Q_N \mathcal{O}_1,
\end{aligned} \tag{3}$$

where $Q_p = 1$, $Q_n = 0$, $g_p = 5.59$, $g_n = -3.83$, $\alpha = 1/137$. The relevant non-relativistic EFT operators \mathcal{O}_i are [11]:

$$\begin{aligned}
\mathcal{O}_1 &= 1, \\
\mathcal{O}_4 &= \vec{S}_\chi \cdot \vec{S}_N, \\
\mathcal{O}_5 &= i \vec{S}_\chi \cdot \left(\frac{\vec{q}}{m_N} \times \vec{v}^\perp \right), \\
\mathcal{O}_6 &= \left(\vec{S}_\chi \cdot \frac{\vec{q}}{m_N} \right) \left(\vec{S}_N \cdot \frac{\vec{q}}{m_N} \right), \\
\mathcal{O}_8 &= \vec{S}_\chi \cdot \vec{v}^\perp, \\
\mathcal{O}_9 &= i \vec{S}_\chi \cdot \left(\vec{S}_N \times \frac{\vec{q}}{m_N} \right), \\
\mathcal{O}_{11} &= i \vec{S}_\chi \cdot \frac{\vec{q}}{m_N},
\end{aligned} \tag{4}$$

where \vec{S}_χ is the DM spin, \vec{S}_N is the nucleon spin, m_N is the nucleon mass, \vec{q} is the momentum exchange, and \vec{v}^\perp is the component of the relative velocity \vec{v}_{rel} orthogonal to \vec{q} .

For the minimal lepton portal dark matter model with the assumption that DM is a fermion, the matched Wilson coefficients for Dirac fermion DM are [5]:

$$\begin{aligned}
(b_\chi)_\ell &= \frac{eQ_\ell |\lambda|^2}{16\pi^2 m_\chi^2} \hat{b}_\chi(\mu, \epsilon), \\
(\mu_\chi)_\ell &= \frac{eQ_\ell |\lambda|^2}{16\pi^2 m_\chi^2} \hat{\mu}_\chi(\mu, \epsilon), \\
(a_\chi)_\ell &= \frac{eQ_\ell |\lambda|^2}{16\pi^2 m_\chi^2} \hat{a}_\chi(\mu, \epsilon), \\
(d_\chi)_\ell &= 0,
\end{aligned} \tag{5}$$

where

$$\begin{aligned}
\hat{b}_\chi(\mu, \epsilon) &= -\frac{1}{24} \left[(8\mu - 8\epsilon + 1) \log \left(\frac{\epsilon}{\mu} \right) \right. \\
&\quad + 4 \left(4 + \frac{\mu + 3\epsilon - 1}{\Delta} \right) \\
&\quad + \frac{2}{\Delta^{3/2}} [8\Delta^2 + (9\mu + 7\epsilon - 5)\Delta \\
&\quad \left. - 4\epsilon(3\mu + \epsilon - 1)] \tanh^{-1} \left(\frac{\Delta^{1/2}}{\mu + \epsilon - 1} \right) \right], \\
\hat{\mu}_\chi(\mu, \epsilon) &= -\frac{1}{2} \left[\frac{1}{2} (\epsilon - \mu) \log \left(\frac{\epsilon}{\mu} \right) - 1 \right. \\
&\quad \left. - \frac{\Delta + \mu + \epsilon - 1}{\Delta^{1/2}} \tanh^{-1} \left(\frac{\Delta^{1/2}}{\mu + \epsilon - 1} \right) \right], \\
\hat{a}_\chi(\mu, \epsilon) &= \frac{1}{12} \left[\frac{3}{2} \log \left(\frac{\epsilon}{\mu} \right) \right. \\
&\quad \left. + \frac{3\mu - 3\epsilon + 1}{\Delta^{1/2}} \tanh^{-1} \left(\frac{\Delta^{1/2}}{\mu + \epsilon - 1} \right) \right],
\end{aligned} \tag{6}$$

with $\mu \equiv m_\phi^2/m_\chi^2$, $\epsilon \equiv m_\mu^2/m_\chi^2$, $\Delta \equiv \mu^2 + (\epsilon - 1)^2 - 2\mu(\epsilon + 1)$ and the charge of muon $Q_l = -1$.

For Majorana fermion DM, the differential rate is obtained by replacing a_χ to $2a_\chi$, while keeping others zero.